ELSEVIER

Cardiovascular Research 70 (2006) 497 – 508

Cardiovascular Research

www.elsevier.com/locate/cardiores

Effects of a Na^+/Ca^{2+} exchanger inhibitor on pulmonary vein electrical activity and ouabain-induced arrhythmogenicity

Wanwarang Wongcharoen [b], Yao-Chang Chen [c], Yi-Jen Chen [a,*], Che-Ming Chang [e], Hung-I Yeh [f], Cheng-I Lin [d], Shih-Ann Chen [b]

[a] *Division of Cardiovascular Medicine, Taipei Medical University, Wan-Fang Hospital, 111, Hsin-Lung Road, Sec. 3, Taipei, Taiwan*
[b] *National Yang-Ming University, School of Medicine, Division of Cardiology, Veterans General Hospital-Taipei, Taipei, Taiwan*
[c] *Department of Biomedical Engineering, Taipei, Taiwan*
[d] *Institute of Physiology and, National Defense Medical Center, Taipei, Taiwan*
[e] *Shin Kong Wu Ho-Su Memorial Hospital and Department of Medicine, Fu Jen Catholic University, Taipei, Taiwan*
[f] *Department of Internal Medicine, Mackay Memorial Hospital, Nursing and Management College, Taipei, Taiwan*

Received 18 October 2005; received in revised form 18 February 2006; accepted 21 February 2006
Available online 3 March 2006
Time for primary review 20 days

Abstract

Objective: Pulmonary veins (PVs) are the most important focus for generation of atrial fibrillation. The Na^+/Ca^{2+} exchange (NCX) current is important in PV electrical activity and cardiac glycosides-induced arrhythmias. The purpose of this study was to investigate whether KB-R7943, a NCX current blocker with preferential inhibition of the Ca^{2+} influx, may alter PV electrophysiological characteristics and reduce glycoside-induced arrhythmogenicity.
Methods: Conventional microelectrodes were used to record the effects of KB-R7943 on action potentials and contractility in isolated rabbit PV tissue specimens with and without administration of ouabain. The ionic currents and intracellular calcium were studied in isolated single cardiomyocytes before and after KB-R7943 by the whole-cell patch clamp and indo-1 fluorimetric ratio techniques.
Results: KB-R7943 (0, 3, 10, 30 μM) concentration-dependently prolonged APD_{50} and APD_{90} and decreased the PV firing rates (2.3 ± 1.2 Hz, 2.1 ± 1.2 Hz, 1.9 ± 0.9 Hz, 1.7 ± 1.1 Hz, $n = 7$, $p < 0.05$) and incidences of delayed afterdepolarizations (DADs). KB-R7943 (3, 30 μM) decreased transient inward currents, Ca^{2+} transient and sarcoplasmic reticulum Ca^{2+} content. Ouabain (0, 0.1, 1 μM) concentration-dependently increased the PV firing rates and DADs in PVs with spontaneous activity ($n = 7$) and induced nonsustained spontaneous activity (1 μM) in the PVs without spontaneous activity ($n = 14$). However, in the presence of KB-R7943 (30 μM), ouabain (1 μM) did not increase the PV firing rates or induce spontaneous activity in the PVs without spontaneous activity ($n = 7$).
Conclusions: KB-R7943 reduces the PV arrhythmogenic activity and prevents the ouabain-induced arrhythmogenicity. Our findings support the role of the NCX current in the PV electrical activity.

Keywords: Atrial fibrillation; Glycosides; Na^+/Ca^{2+} exchange current; Pulmonary vein; Triggered activity

1. Introduction

Atrial fibrillation (AF) is the most common sustained arrhythmia in clinical medicine. The pulmonary veins (PVs) have been demonstrated to be an important source of the initiation of AF [1,2] and also to have a role in the maintenance of AF [3]. The PVs are known to contain cardiomyocytes with and without pacemaker activity and are suggested to be subsidiary pacemakers [4,5]. Through several mechanisms, PVs have been found to have a high arrhythmogenic potential to induce atrial arrhythmias [6–12]. However, the pathophysiology underlying the arrhythmogenesis of the PVs has not been fully elucidated. Previous studies have indicated that abnormal calcium regulation and triggered activity may underlie PV arrhyth-

* Corresponding author. Fax: +886 2 29339378; +886 2 28735656.
E-mail address: a9900112@ms15.hinet.net (Y.-J. Chen).

0008-6363/$ - see front matter © 2006 European Society of Cardiology. Published by Elsevier B.V. All rights reserved.
doi:10.1016/j.cardiores.2006.02.026

mogenic acitivity [13,14]. Honjo et al. [13] demonstrated that Na^+–Ca^{2+} exchanger (NCX) blockers abolished PV electrical activity during rapid pacing in ryanodine treated PVs. Our previous studies have shown that activation of transient inward currents (I_{ti}) with the genesis of delayed afterdepolarizations (DADs) is important for the PV electrical activity [7,11]. It is known that NCX plays a pivotal role in the genesis of I_{ti} and repetitive activity of cardiomyocytes [12]. These findings indicated the importance of the NCX currents in PV arrhythmogenic activity. KB-R7943 is a novel isothiourea derivative that has been reported to preferentially block the Ca^{2+} influx (reverse) mode of the NCX current [15,16]. Several studies have shown that KB-R7943 may eliminate the ischemia and reperfusion-induced arrhythmias [17,18]. Furthermore, through the prevention of atrial electrical remodeling, KB-R7943 was demonstrated to reduce AF in the canine model and was suggested to be a potentially antiarrhythmic agent [19]. Therefore, it is possible that KB-R7943 may inhibit PV arrhythmogenic activity and reduce the occurrence of AF.

Cardiac glycosides are frequently used in the treatment of heart failure with and without AF. However, the narrow therapeutic range of the cardiac glycosides has resulted in easily inducing cardiac arrhythmias due to intoxication. Cardiac glycosides, such as ouabain may increase the intracellular Ca^{2+} with the enhancement of the NCX currents through the inhibition of the Na^+/K^+-ATPase. These effects may shorten the atrial refractory period and aggravate tachycardia-induced atrial electrical remodeling with a predisposition for AF [20,21]. Moreover, it has been reported that cardiac glycosides enhanced PV arrhythmogenic activity and induced atrial tachyarrhythmias in guinea pig [22]. KB-R7943 has been shown to prevent the arrhythmogenic effect of cardiac glycosides [23,24]. It is possible that KB-R7943 may prevent glycoside-induced PV arrhythmogenesis. The purposes of the present study were to investigate the effects of KB-R7943 on the PV electrical activity and evaluate whether KB-R7943 may reduce the ouabain-induced PV arrhythmogenicity.

2. Methods

2.1. Rabbit PV tissue preparations

The investigation conformed to the institutional Guide for the Care and Use of Laboratory Animals. Rabbits (weight, 1–2 kg) were anesthetized with an intraperitoneal injection of sodium pentobarbital (40 mg/kg). A mid-line thoracotomy was then performed and the heart with the lungs was removed. For dissection of the PVs, the left atrium was opened by an incision along mitral valve annulus extending from the coronary sinus to the septum in Tyrode's soluton with a composition (in mM) of 137 NaCl, 4 KCl, 15 $NaHCO_3$, 0.5 NaH_2PO_4, 0.5 $MgCl_2$, 2.7 $CaCl_2$, and 11 dextrose. The PVs were separated from the atrium at the left atrium-PV junction and separated from the lungs at the ending of the PV myocardial sleeves. One end of the preparation, consisting of the PVs and atrium-PV junction, was pinned with needles to the bottom of a tissue bath. The other end was connected to a Grass FT03C force transducer with a silk thread. The adventitia of the PVs faced upwards. The tissue was superfused at a constant rate (3 ml/min) with Tyrode's solution which was saturated with a 97% O_2–3% CO_2 gas mixture. The temperature was maintained constant at 37 °C and the preparations were allowed to equilibrate for 1 h before the electrophysiological study.

2.2. Electrophysiological and pharmacological studies

The transmembrane action potential (AP) of the PVs was recorded by means of machine-pulled glass capillary microelectrodes filled with 3 M of KCl and the PV preparation was connected to a WPI model FD223 electrometer under tension with 150 mg. The electrical and mechanical events were displayed simultaneously on a Gould 4072 oscilloscope and Gould TA11 recorder. The signals were recorded with DC coupling and a 10-KHz low-pass filter cutoff frequency using a data acquisition system. Signals were recorded digitally with 16-bit accuracy at a rate of 125 kHz. An electrical stimuli with a 10-ms duration and suprathreshold strength (30% above the threshold) were provided by a Grass S88 stimulator through a Grass SIU5B stimulus isolation unit. Different concentrations of KB-R7943 (0, 0.3, 3, 10, 30 μM) or ouabain (0.1, 1 μM) were sequentially superfused to test the pharmacological responses. The PV preparations were treated with either or both drugs for at least 20 min for each concentration. The 90% and 50% AP durations (APD_{90}, APD_{50}), AP amplitude (APA), potential during the pleateau of the AP and contractile force were measured during 2 Hz electrical stimuli before and after the drug administration.

2.3. Electropharmacological study in single PV cardiomyocytes

PV cardiomyocytes from rabbits were enzymatically dissociated through the same procedure as previously described [11]. PV cardiomyocytes with pacemaker activity were identified by the presence of constantly spontaneous beating during perfusion with Tyrode's solution with a composition (in mM) of NaCl 137, KCl 5.4, HEPES 10, $MgCl_2$ 0.5, $CaCl_2$ 1.8, and glucose 10.

A whole-cell patch-clamp was performed in the PV cardiomyocytes with pacemaker activity before and after the administration of KB-R7943 by an Axopatch 1D amplifier (Axon Instruments, California, USA) at 35±1 °C as previously described [25]. The ionic currents were recorded in the voltage-clamp mode [7,8]. Micropipettes were filled with a solution containing (in mM) CsCl 130, $MgCl_2$ 1,

Mg_2ATP 5, HEPES 10, EGTA 10, NaGTP 0.1, and Na_2 phosphocreatine 5 (pH of 7.2 with CsOH) for L-type calcium current (I_{Ca-L}); containing (in mM) NaCl 20, CsCl 110, $MgCl_2$ 0.4, $CaCl_2$ 1.75, TEACl 20, BAPTA 5, glucose 5, Mg_2ATP 5, and HEPES 10 (pH of 7.25 with CsOH) for NCX current; containing (in mM) CsCl 133, NaCl 5, EGTA 10, Mg_2ATP 5, TEACl 20, HEPES 5 (pH 7.3 with CsOH) for Na^+ current (I_{Na}); and containing (in mM) KCl 20, K

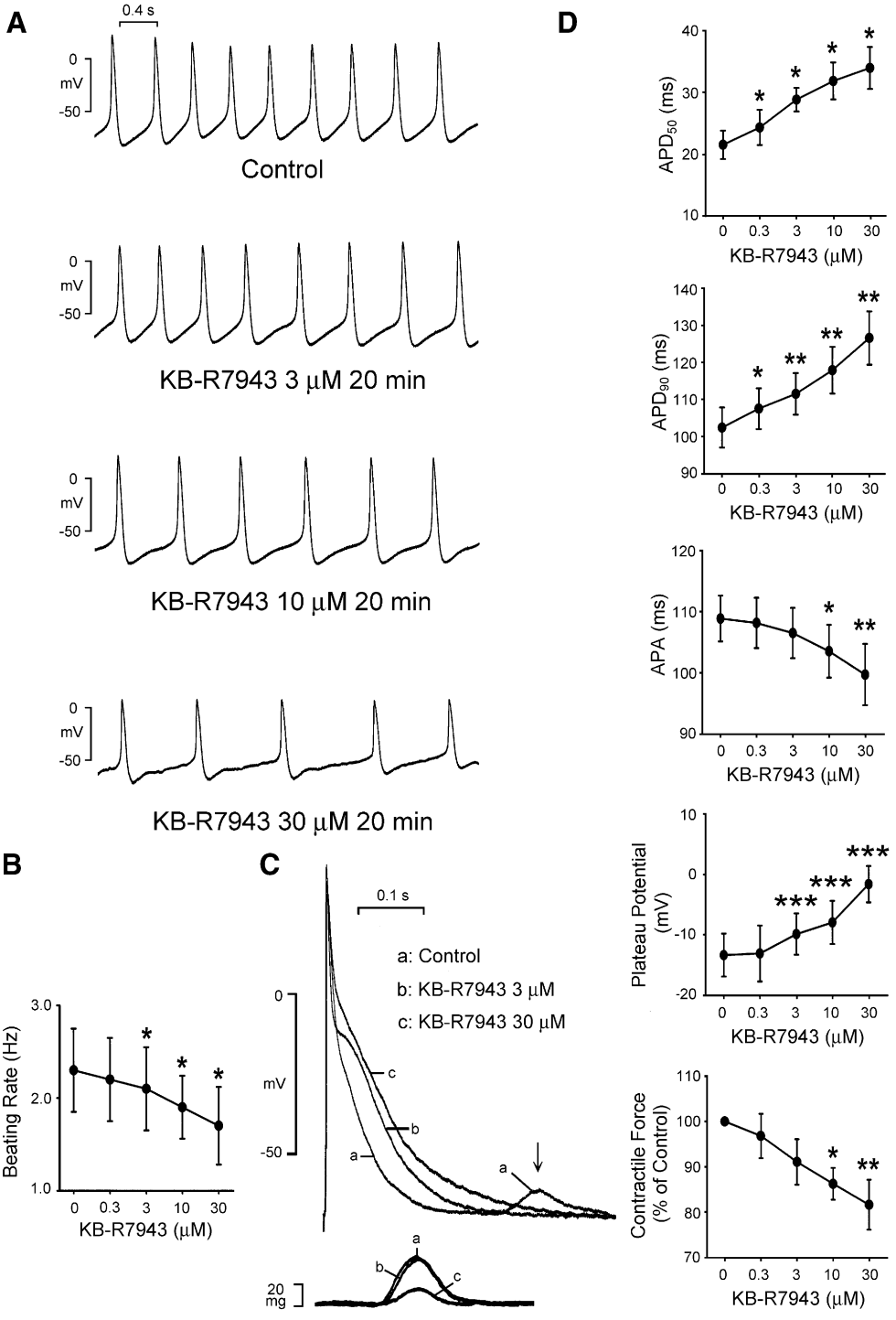

Fig. 1. Effects of KB-R7943 on the PV electrical activity. Panel A shows the tracings of the effects of different concentrations of KB-R7943 on the firing rates in the PVs with spontaneous activity. Panel B shows the concentration–response curve of the effects of KB-R7943 on the PV firing rate ($n=7$). Panel C shows the superimposed tracings of different concentrations of KB-R7943 on the AP configuration and contractile force. The effect of KB-R7943 on the suppression of DADs (↓) is shown. Panel D shows the concentration–response curve of the effects of KB-R7943 on the APD_{50}, APD_{90}, APA, potential during plateau phase of AP (plateau potential) and contractile force ($n=8$). *$P<0.05$, **$P<0.01$, and ***$P<0.001$ versus before the KB-R7943 administration.

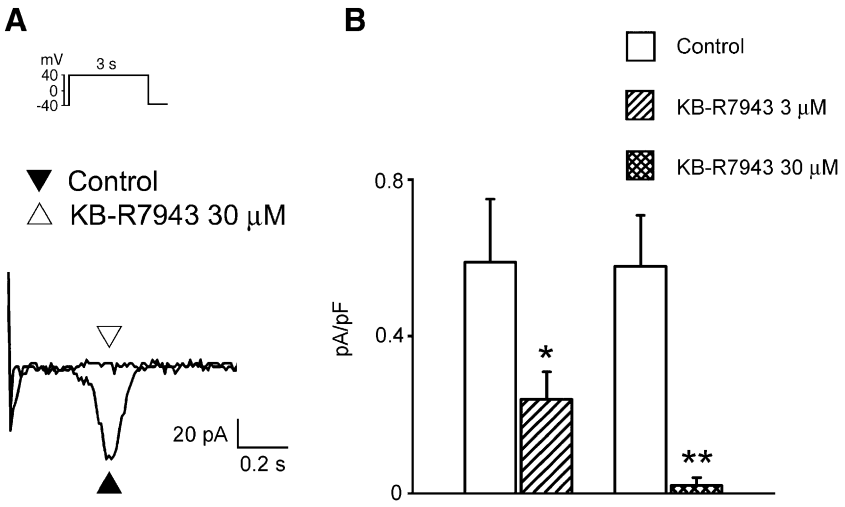

Fig. 2. Effects of KB-R7943 on transient inward currents. Panel A shows the tracings of the I_{ti} before and after the administration of KB-R7943 (30 μM) in PV cardiomyocytes. Panel B shows the average of I_{ti} before and after KB-R7943 (3 μM, $n=7$; 30 μM, $n=7$). *$P<0.05$ and **$P<0.01$ versus before the KB-R7943 administration. The inset in the current traces shows the clamp protocol.

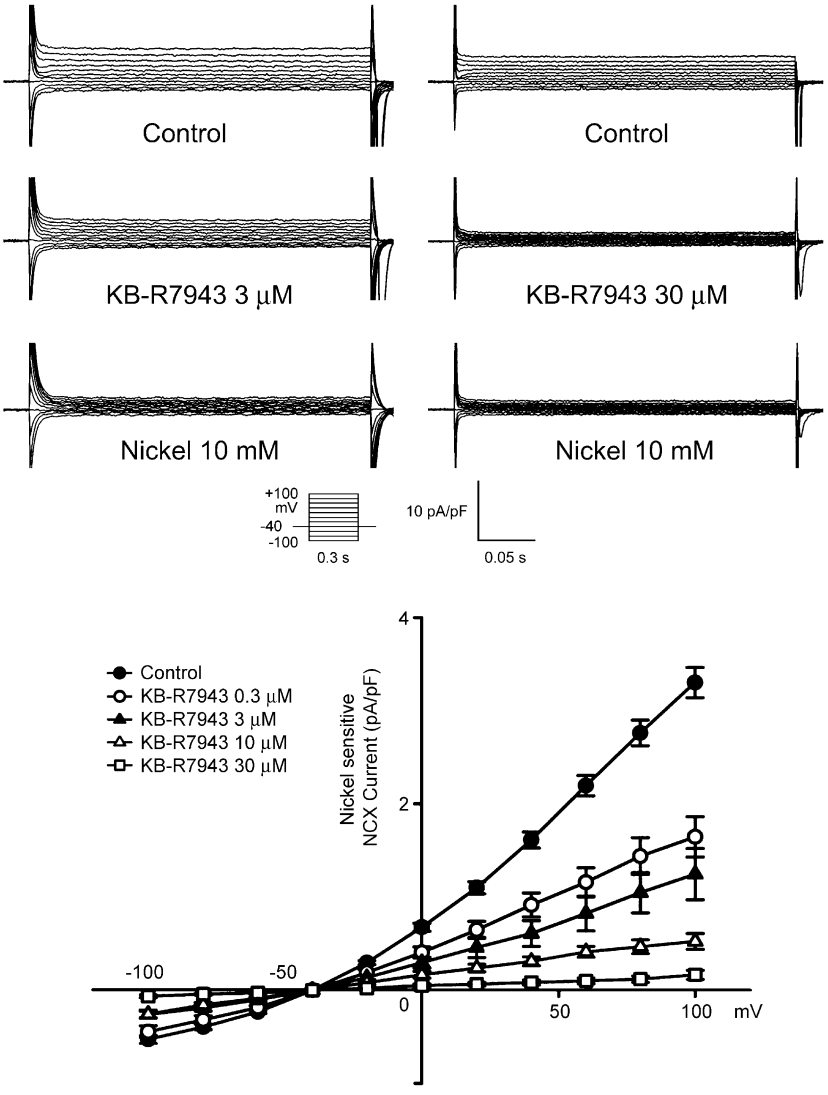

Fig. 3. The tracings and $I-V$ relationship of NCX currents before and after the administration of KB-R7943 (control, $n=34$; KB-R7943, 0.3 μM, $n=10$; 3 μM, $n=8$; 10 μM, $n=8$; and 30 μM, $n=8$) in the PV cardiomyocytes. The insets in the current traces show the various clamp protocols.

aspartate 110, $MgCl_2$ 1, Mg_2ATP 5, HEPES 10, EGTA 0.5, LiGTP 0.1, and Na_2 phosphocreatine 5 (pH of 7.2 with KOH) for I_{ti} and potassium currents.

I_{Ca-L} was recorded during depolarization from a holding potential of −50 mV to testing potentials ranging from −40 to +60 mV in 10-mV steps for 300 ms at a frequency of 0.1 Hz by means of perforated patch-clamp with amphotericin B. The NaCl and KCl in the external solution were replaced by TEACl and CsCl, respectively.

I_{Na} was recorded during depolarization from a holding potential of −120 mV to testing potentials ranging from −90 to +60 mV in 10-mV steps for 40 ms at a frequency of 3 Hz at room temperatures (22–24 °C) with an external solution containing (in mM): NaCl 5, CsCl 133, $MgCl_2$ 2, $CaCl_2$ 1.8, nifedipine 0.002, HEPES 5 and glucose 5 with a pH of 7.3.

The transient outward current (I_{to}) was studied with a double-pulse protocol. A 30-ms pre-pulse from −80 to −40 mV was used to inactivate the sodium channels, followed by a 300-ms test pulse to +60 mV in 10-mV steps at a frequency of 0.1 Hz. $CdCl_2$ (200 μM) was added to the bath solution to inhibit I_{Ca-L}. I_{to} was measured as the difference between the peak outward current and steady state current. The delayed rectified outward potassium current (I_K) was measured from the peak outward current at the end of 1 s of the depolarization from −40 to +60 mV in 10-mV steps at a frequency of 0.1 Hz during the infusion of $CdCl_2$ (200 μM) and 4-aminopyridine (2 mM) in the bath solution.

I_{ti} was induced during depolarization from a holding potential of −40 mV to +40 mV for a duration of 3 s and the current was measured on the return to −40 mV. The amplitude of the I_{ti} was measured as the difference between the peak of the transient current and mean of the current just before and after the transient current [7,11].

The inward rectifier potassium current (I_{K1}) was activated from −40 mV to test potentials ranging from −20 to −120 mV in 10-mV steps for 1 s at a frequency of 0.1 Hz under the infusion of $CdCl_2$ (200 μM) and 4-aminopyridine (2 mM) in the bath solution. The amplitudes of the I_{K1} were measured as 1 mM barium-sensitive currents.

The NCX current was elicited by depolarization in 10 mV steps from a holding potential of −40 mV to test potentials from −100 to +100 mV for 300 ms at a frequency of 0.1 Hz (insets in Fig. 3). The amplitudes of the NCX current were measured as 10 mM nickel-sensitive currents. The external solution (in mM) consisted of NaCl 140, $CaCl_2$ 2, $MgCl_2$ 1, HEPES 5 and glucose 10 with a pH of 7.4 and contained strophanthidin (10 μM), nitrendipine (10 μM) and niflumic acid (100 μM) [25].

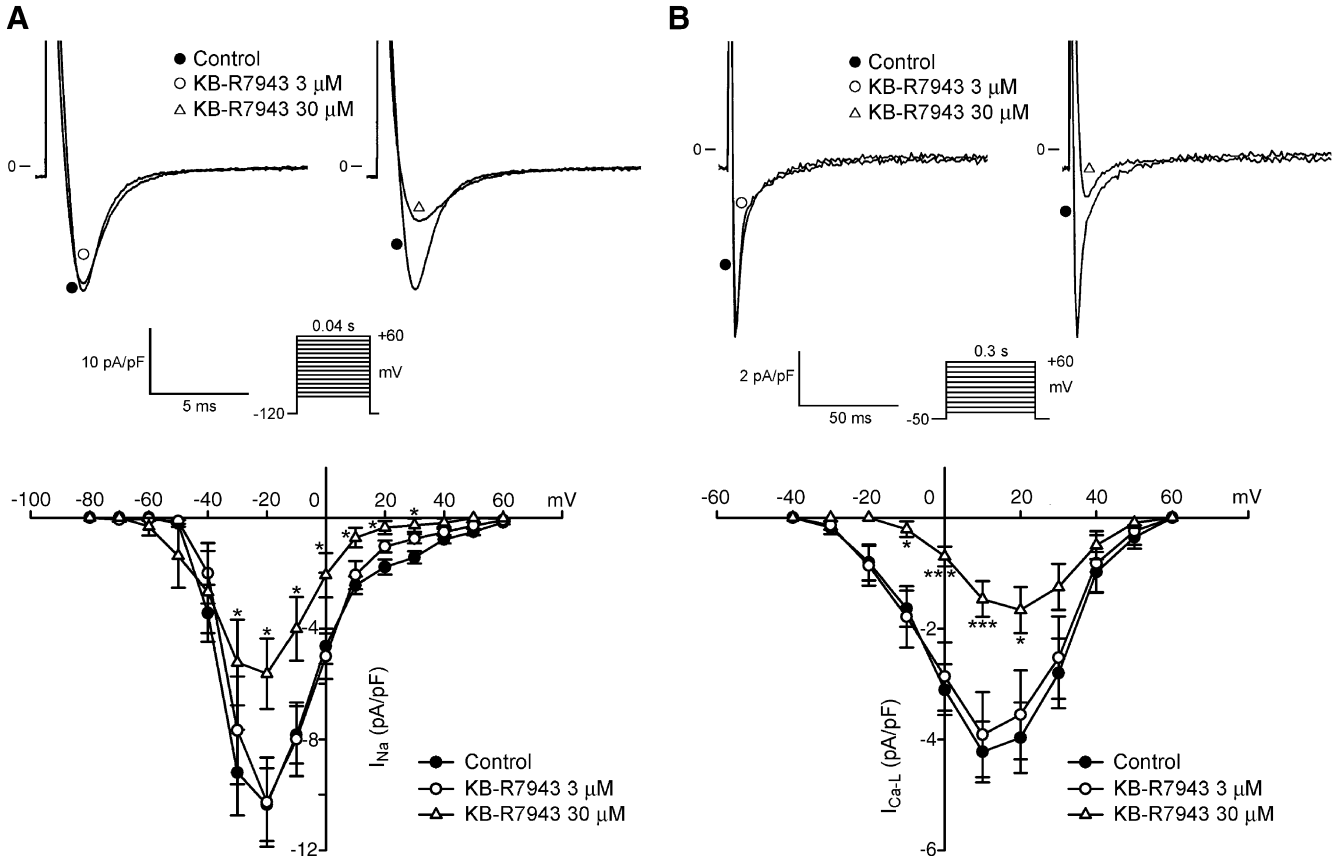

Fig. 4. Effects of KB-R7943 on I_{Na} and I_{Ca-L}. Panel A shows the tracings and $I-V$ relationship of I_{Na} before and after 3 μM ($n=10$) and 30 μM ($n=9$) KB-R7943 in the PV cardiomyocytes. Panel B shows the tracings and $I-V$ relationship of I_{Ca-L} before and after 3 μM ($n=7$) and 30 μM ($n=7$) KB-R7943 in the PV cardiomyocytes. *$P<0.05$ and ***$P<0.001$ versus before the KB-R7943 administration. The insets in the current traces show the clamp protocol.

2.4. Measurement of the intracellular calcium

Intracellular calcium ($[Ca^{2+}]_i$) was recorded by a fluorimetric ratio technique. The fluorescent indicator indo-1 was loaded by incubating the myocytes at room temperature for 20–30 min with 25 μM of indo-1/AM (Sigma Chemical, St. Louis, MO). The PV cardiomyocytes were then perfused with a normal bath solution at 35±1 °C for at least 20 min to wash out the extracellular indicator and to allow for intracellular deesterification of the indo-1. The background and cell autofluorescence were cancelled out by zeroing the output of the photomultiplier tubes using cells without indo-1 loading. The experiments were performed during superfusion before and after KB-R7943.

Ultraviolet light at a strength of 360 nm with a monochromator was used for the excitation of the indo-1 from a xenon arc lamp controlled by a microfluorometry system (OSP100-CA, Olympus, Tokyo, Japan) and the excitation light beam was directed into an inverted microscope (IX-70; Olympus). The emitted fluorescence signals from the indo-1/AM loaded myocytes were digitized at 200 Hz. The ratio of flurorescence emissions at 410 nm and 485 nm was recorded. $R_{410/485}$ was used as the index of the $[Ca^{2+}]_i$. This approach avoided the uncertainties related to in vivo calibration of the fluorescent

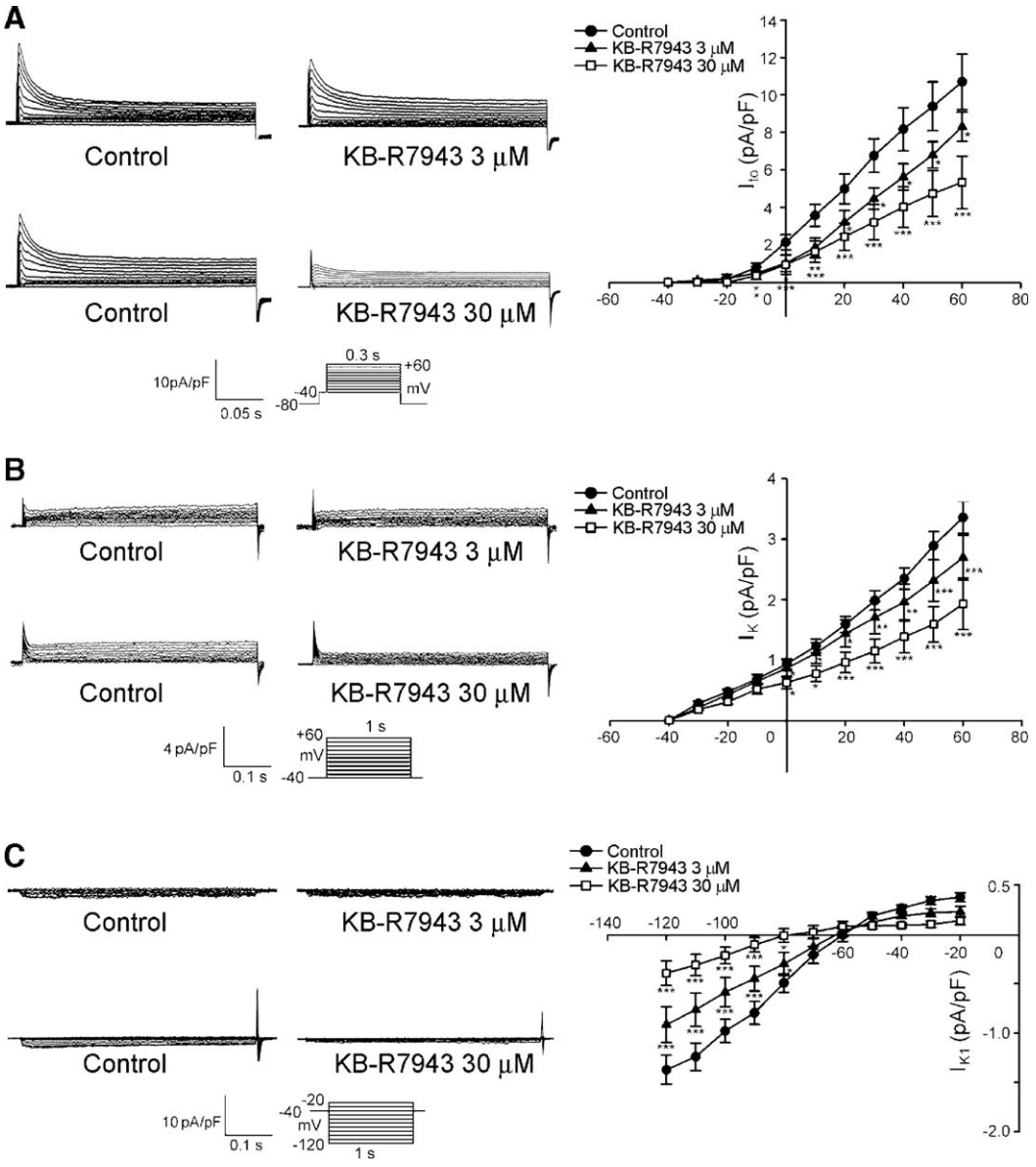

Fig. 5. Effects of KB-R7943 on I_{to}, I_K and I_{K1}. Panel A shows the tracings and $I-V$ relationship of Ito before and after 3 μM ($n=7$) and 30 μM ($n=7$) KB-R7943 in the PV cardiomyocytes. Panel B shows the tracings and $I-V$ relationship of I_K before and after 3 μM ($n=12$) and 30 μM ($n=10$) KB-R7943 in the PV cardiomyocytes. Panel C shows the tracings and $I-V$ relationship of I_{K1} before and after 3 μM ($n=7$) and 30 μM ($n=7$) KB-R7943 in the PV cardiomyocytes. *$P<0.05$, **$P<0.01$ and ***$P<0.001$ versus before the KB-R7943 administration. The insets in the current traces show the various clamp protocols.

Ca^{2+} indicators. The Ca^{2+} transient, peak systolic $[Ca^{2+}]_i$, diastolic $[Ca^{2+}]_i$, and decay portion of the Ca^{2+} transient (τ_{Ca}) were measured during a 2 Hz field-stimulation with 10-ms twice-threshold strength square-wave pulses. The τ_{Ca} was determined by the mono-exponential least-squares fit. The fluorescence ratio data were processed and stored in a computer using software (OSP-SFCA; Olympus). Sarcoplasmic reticulum (SR) Ca^{2+} content was estimated by adding 20 mM caffeine after electric stimulation at 2 Hz for at least 30 s. The total SR Ca^{2+} content was measured from the peak amplitude of the caffeine-induced Ca^{2+} transients.

2.5. Statistical analysis

All quantitative data are expressed as mean ± SEM. A paired *t*-test was used to compare the differences before and after the drug administration in the PV tissue preparations

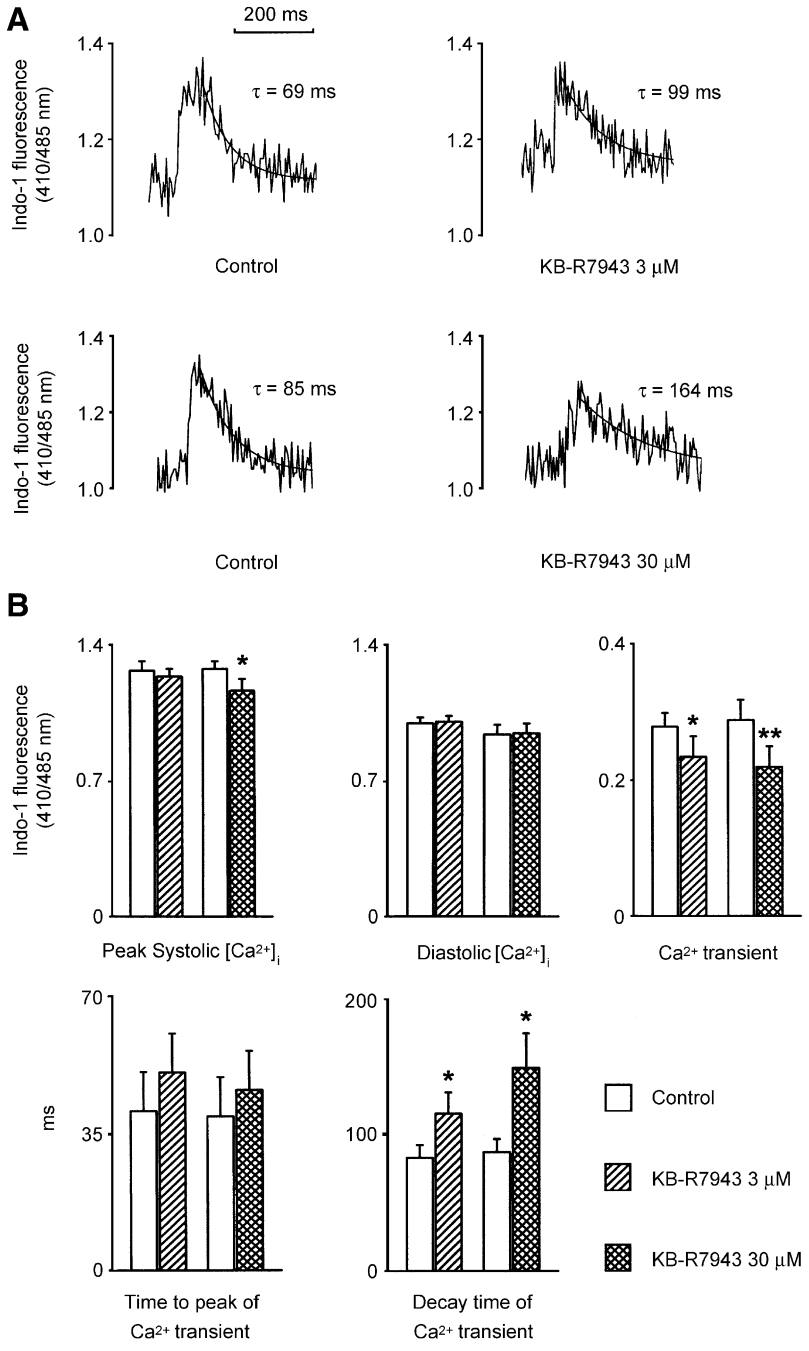

Fig. 6. Effects of KB-R7943 on the Ca^{2+} transient in the PV cardiomyocytes. Panel A shows the tracings of the Ca^{2+} transient before and after KB-R7943 (3, 30 μM) administration. Panel B shows the average of the peak systolic $[Ca^{2+}]_i$, diastolic $[Ca^{2+}]_i$, Ca^{2+} transient, time to the peak, and decay portion of the Ca^{2+} transient (τ_{Ca}) before and after 3 μM ($n=7$) and 30 μM ($n=7$) KB-R7943 (3, 30 μM). *$P<0.05$, and **$P<0.01$ versus before the KB-R7943 administration.

and single cardiomyocytes. Nominal variables were compared by a Chi-square analysis with Yates correction or Fisher's exact test. A p-value lower than 0.05 was considered statistically significant.

3. Results

3.1. Effects of KB-R7943 on the PV electrical activity

As the examples show in Fig. 1A, KB-R7943 (3, 10, 30 μM) concentration-dependently decreased the firing rates in the PVs with spontaneous activity (Fig. 1B). In the PVs without spontaneous activity, KB-R7943 concentration-dependently prolonged the APD_{50} and APD_{90} and KB-R7943 (10, 30 μM) decreased the APA significantly (Fig. 1C, D). Additionally, KB-R7943 (3, 10, 30 μM) concentration-dependently shifted the plateau potential to less negative values. KB-R7943 (10, 30 μM) decreased the contractile force of the PVs, but did not affect the diastolic tension (Fig. 1C, D). Moreover, KB-R7943 (0, 0.3, 3, 10, 30 μM) concentration-dependently decreased the incidence of DADs ($n=11$; 45%, 45%, 18%, 0%, 0%, $p<0.05$) significantly.

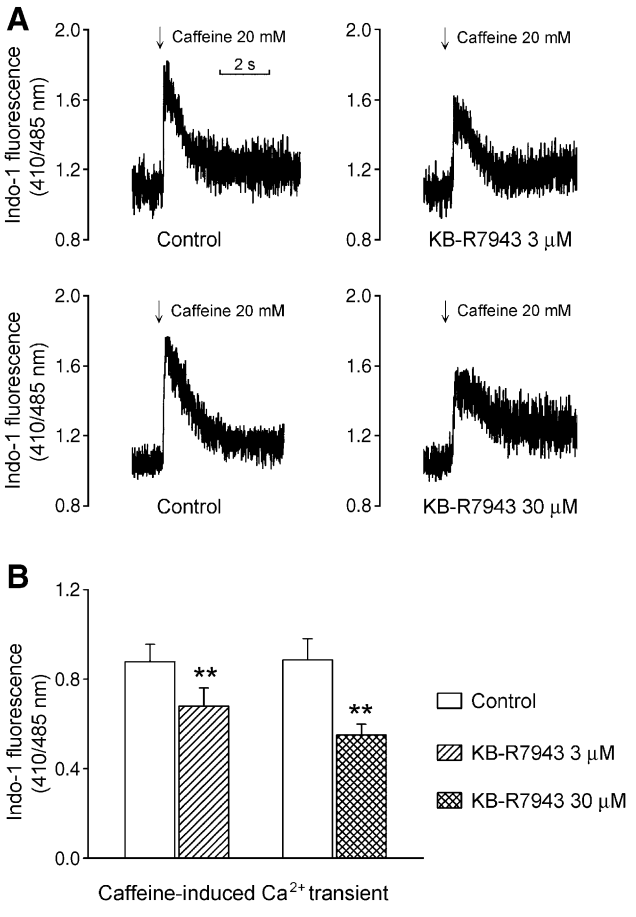

Fig. 7. Effects of KB-R7943 on SR Ca^{2+} content. Panel A shows the tracings of caffeine-induced Ca^{2+} transient before and after KB-R7943 (3, 30 μM) administration. Panel B shows the average of SR Ca^{2+} content before and after 3 μM ($n=7$) and 30 μM ($n=7$) KB-R7943. $^{**}P<0.01$ versus before the KB-R7943 administration.

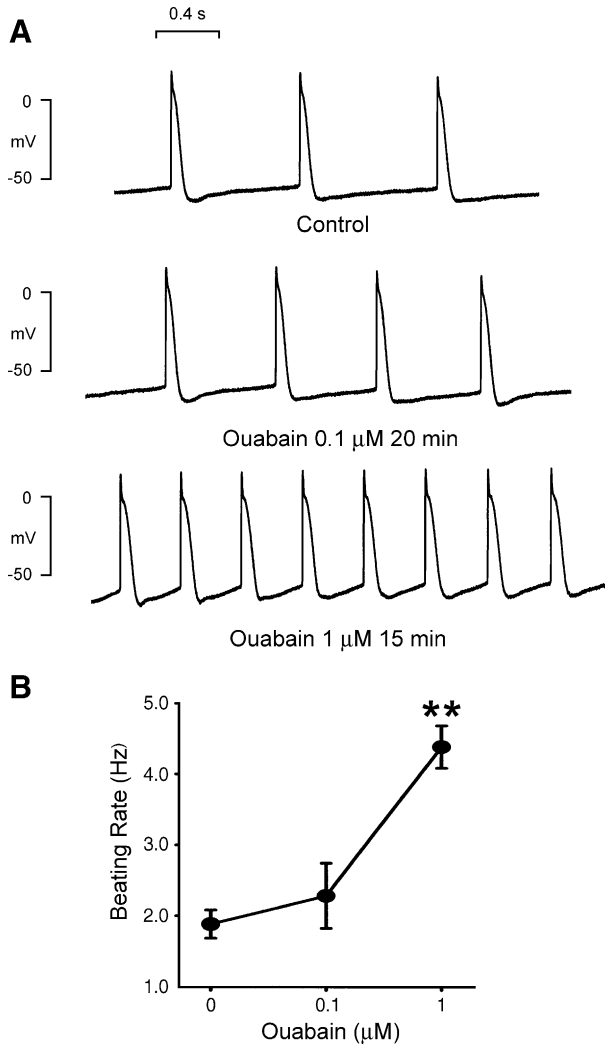

Fig. 8. The effects of ouabain on the PVs with spontaneous activity. (A) The tracings show that ouabain (0.1, 1 μM) increased the firing rates in the PVs. (B) The concentration–response curve of the effects of ouabain on the PV firing rate ($n=7$). $^{**}P<0.01$ versus before the ouabain administration.

3.2. Effect of KB-R7943 on the membrane currents of PV cardiomyocytes

As the examples show in Fig. 2, KB-R7943 significantly decreased I_{ti} by 59% at 3 μM and by 96% at 30 μM (Fig. 2B). Fig. 3 shows the tracings and $I-V$ relationship of the effects of KB-R7943 on NCX currents of PV cardiomyocytes. KB-R7943 reduced the reverse mode of NCX currents with an IC_{50} of 0.36 μM and reduced the forward mode of NCX with an IC_{50} of 5.62 μM. Therefore, KB-R7943 preferentially suppressed the reverse mode of NCX currents in PV cardiomyocytes.

Fig. 4 shows the tracings and $I-V$ relationship of the effects of KB-R7943 (3, 30 μM) on I_{Na} (Fig. 4A) and I_{Ca-L}

(Fig. 4B) of the PV cardiomyocytes. KB-R7943 (30 μM, but not 3 μM), decreased I_{Ca-L} and I_{Na} significantly.

Fig. 5 shows the tracings and $I-V$ relationship of the effects of KB-R7943 (3, 30 μM) on I_{to} (Fig. 5A), I_K (Fig. 5B) and I_{K1} (Fig. 5C) of the PV cardiomyocytes. KB-R7943 (3, 30 μM) reduced the I_{to}, I_K and I_{K1} significantly.

3.3. Effects of KB-R7943 on the intracellular calcium in PV cardiomyocytes

As the examples show in Fig. 6A, KB-R7943 (3, 30 μM) decreased the Ca^{2+} transient and prolonged the decay time of the Ca^{2+} transient. However, only KB-R7943 (30 μM) significantly decreased the peak systolic $[Ca^{2+}]_i$. Fig. 6B shows the average data of the effect of KB-R7943 (3, 30 μM) on the peak systolic $[Ca^{2+}]_i$, diastolic $[Ca^{2+}]_i$, Ca^{2+} transient, time to peak of Ca^{2+} transient and decay time of Ca^{2+} transient. In addition, KB-R7943 decreased SR Ca^{2+} content by 23% at 3 μM and by 38% at 30 μM (Fig. 7).

3.4. Effects of ouabain on the PV electrical activity

Fig. 8A shows an example of ouabain's effect on the PVs with spontaneous activity. Ouabain (0, 0.1, 1 μM) concentration-dependently increased the PV firing rates (Fig. 8B). In the PVs without spontaneous activity, ouabain (1 μM) induced PV nonsustained spontaneous activity in 13 (93%) of 14 PVs (Fig. 9A) after the drug administration for

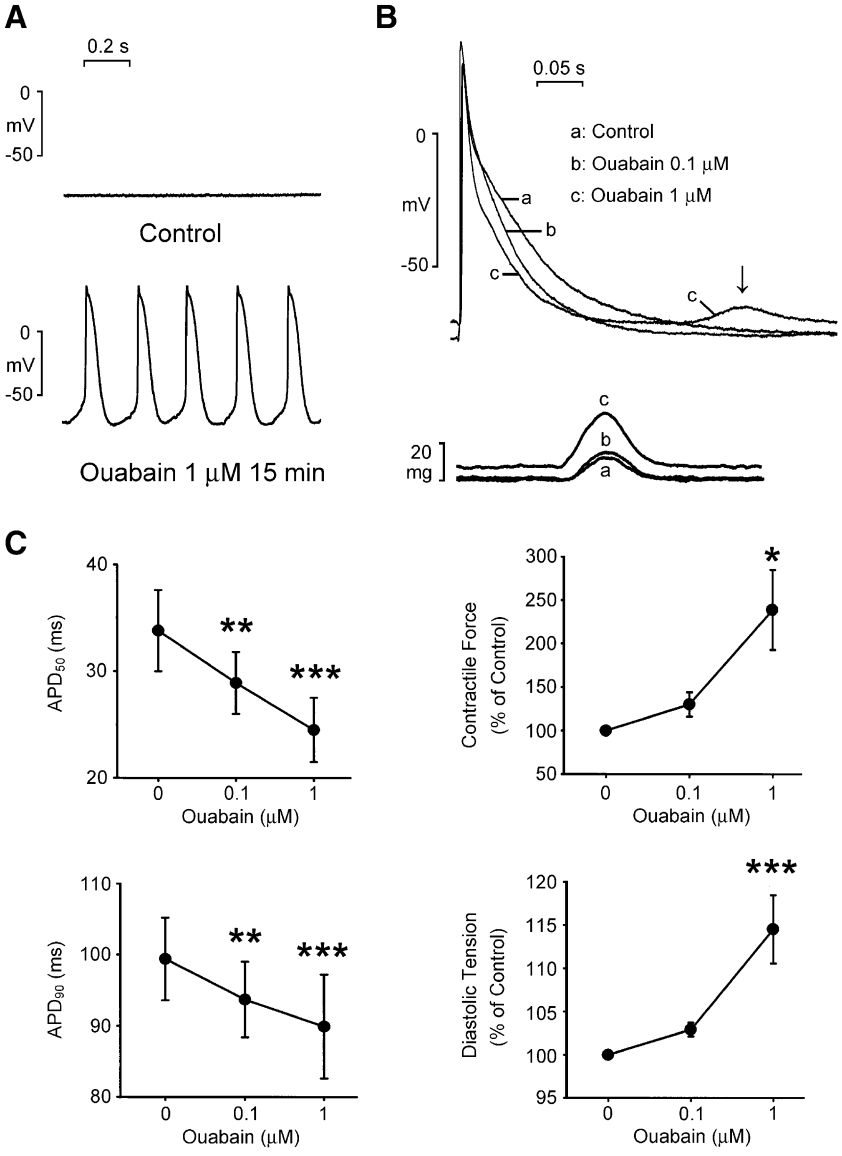

Fig. 9. Effects of ouabain on the PVs without spontaneous activity. (A) The tracings show an example of ouabain (1 μM) induced PV firing in a PV without spontaneous activity. The development of a phase 4 depolarization was noted. (B) The superimposed tracings show the effects of ouabain (0.1, 1 μM) on the AP configuration and contractile force. Note that ouabain (1 μM) induced a DAD (↓) and increased the contractile force and diastolic tension. C, The concentration–response curve of the effects of ouabain on the APD50 and APD90, contractile force and diastolic tension ($n=11$). *$P<0.05$, **$P<0.01$, and ***$P<0.001$ versus before the ouabain administration.

11±3 min, and ouabain (0, 0.1, 1 μM) increased the incidences of DADs (Fig. 9B, $n=14$; 43% versus 57% versus 93%, $p<0.05$). However, ouabain at 0.1 μM did not induce spontaneous activity in any PV tissue preparations. Moreover, ouabain (0.1, 1 μM) concentration-dependently decreased the APD_{50} and APD_{90} (Fig. 9B and C). Ouabain (1 μM, but not 0.1 μM) increased the contractile force and diastolic tension (tonotropic effect) significantly (Fig. 9B). The effects of ouabain were also investigated in isolated left atrial tissue preparations. Compared to that in the PVs, ouabain (1 μM) induced left atrial spontaneous activity with a lower incidence (34%, $n=35$, $p<0.05$).

3.5. Effect of KB-R7943 on the ouabain-induced arrhythmogenicity

In the presence of KB-R7943 (30 μM), ouabain (1 μM) did not increase the firing rates in the PV with spontaneous activity but decreased it from 1.8±0.4 Hz to 1.4±0.3 Hz (Fig. 10A, $n=7$, $p<0.05$). In the PVs without spontaneous activity, ouabain (1 μM) only induced spontaneous activity in 2 (25%) of 8 PVs pretreated with KB-R7943 (30 μM), which was significantly lower than that without the presence of KB-R7943 ($p<0.05$). The average time (24±2 versus 11±3 min) for ouabain-induced PV spontaneous activity was longer in the PVs pretreated with KB-R7943 than in those without. Moreover, in the presence of KB-R7943 (30 μM), the effects of ouabain (1 μM) on the APD_{50} (33±4 to 30±4 ms, $p>0.05$) and APD_{90} (131±7 to 125±8 ms, $p>0.05$) were insignificant and the positive tonotropic effect of ouabain was significantly reduced. However, the positive inotropic effect was not affected (Fig. 10B).

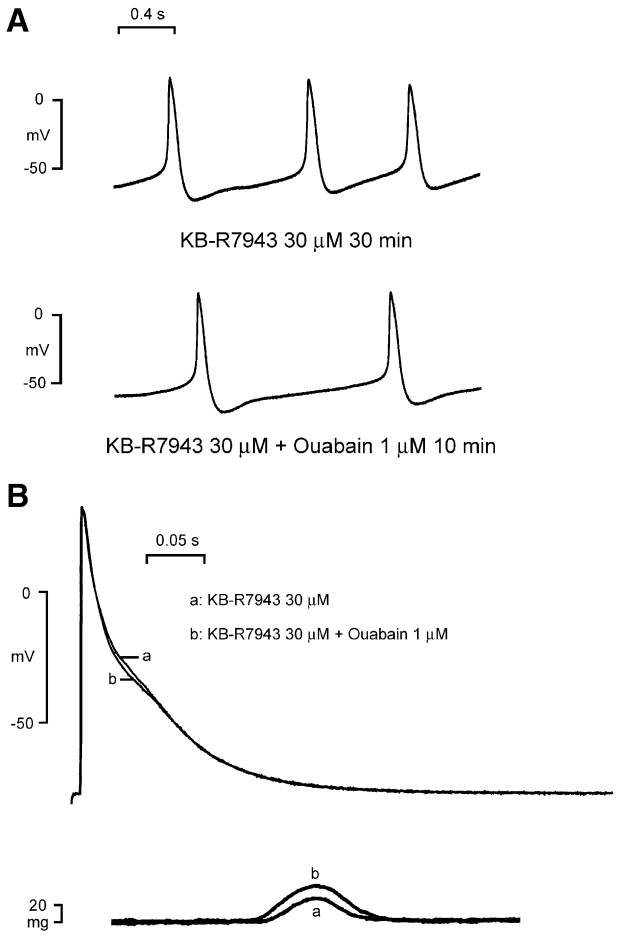

Fig. 10. Interactions of KB-R7943 and ouabain on the PV electrical activity. (A) Ouabain did not increase, but decrease the PV firing rates in the presence of 30 μM KB-R7943. (B) Effects of ouabain on the AP configuration, contractile force and diastolic tension in the presence of 30 μM KB-R7943. The positive tonotropic effect was significantly reduced but the positive inotropic effect was not affected.

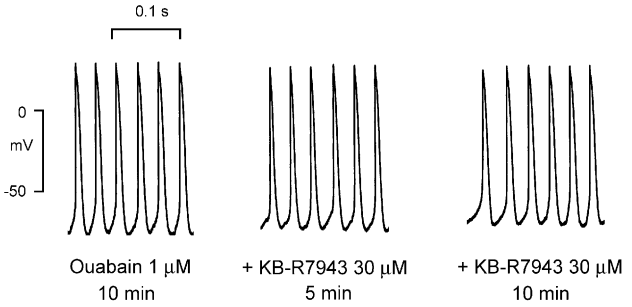

Fig. 11. Effects of KB-R7943 on ouabain-induced arrhythmias. The tracings show that KB-R7943 (30 μM) did not terminate the ouabain (1 μM)-induced arrhythmogenic activity.

In the presence of KB-R7943 (30 μM), ouabain (1 μM) significantly increased the contractile force in a comparable degree as ouabain without KB-R7943 (191±67% versus 239±47%, $p>0.05$).

This study also investigated the effects of KB-R7943 on ouabain-induced arrhythmias. After ouabain (1 μM)-induced PV arrhythmogenic activity ($n=7$), KB-R7943 (30 μM) did not significantly change the firing rates (3.6±0.3 versus 3.7±0.4, $p>0.05$, Fig. 11).

4. Discussion

4.1. Effects of NCX inhibitors on the PV electrical activity

Abnormalities in intracellular Ca^{2+} homeostasis are important in the pathophysiology of AF [26]. NCX induces I_{ti} with the genesis of DADs, and an upregulation of NCX has been found in atrial myocytes in AF patients [27]. In this study, we studied the effect of NCX blockers on the PV electrical activity and found that KB-R7943 reduced PV arrhythmogenic activity with the suppression of the I_{ti}, DADs and PV spontaneous activity. Consistent with other studies, the present study showed that KB-R7943 selectively inhibited the NCX currents preferentially on the reverse mode rather than the forward mode [15,17]. The IC_{50} of the reverse mode in the PVs was similar to the previous study on guinea-pig ventricular cells [15].

Similarly, KB-R7943 was found to have effects on other ionic currents [15,16]. KB-R7943 at 3 μM reduced I_{to}, I_K, I_{K1} and SR Ca^{2+} content and KB-R7943 at 30 μM reduced I_{Na}, I_{Ca-L}, I_{to}, I_K, I_{K1} and SR Ca^{2+} content.

In this study, KB-R7943, both at low and high concentrations, reduced PV arrhythmogenicity through its effects on the triggered activity and automaticity. The effects of KB-R7943 on the decrease of DADs, I_{ti} and PV firing rates could be caused by the reduction in the SR Ca^{2+} content due to the decrease in the Ca^{2+} entry during AP, either from inhibition of the reverse mode of the NCX currents (3, 30 μM) or the inhibition of I_{Ca-L} (30 μM). DADs have been proposed to be caused by diastolic Ca^{2+} release from SR. It has been demonstrated that the SR Ca^{2+} content determined the spontaneous diastolic Ca^{2+} release and influenced the pacemaker rates [28]. As the SR Ca^{2+} content reduced, there would be no longer a diastolic Ca^{2+} release, which would result in a decrease of DADs. The decrease in spontaneous diastolic Ca^{2+} release by KB-R7943 also would prolong the diastolic depolarization period and reduce the PV firing rates. In addition, the direct inhibitory effect of high dose of KB-R7943 on the forward mode of NCX currents may also have a role in the decrease of DADs, I_{ti} and PV firing rates. However, it is not clear to what extent the reduction was related to either of these mechanisms. Moreover, the superior antiarrhythmic effect of a higher dose of KB-R7943 may also arise from the nonspecific actions on several ion currents. The reduction in the SR Ca^{2+} content could also explain the decrease in the Ca^{2+} transient and a negative inotropic effect caused by KB-R7943. The prolongation of the calcium decay by KB-R7943 (30 μM) suggested that the calcium extrusion through the NCX currents was reduced.

Previous studies have shown that NCX currents were similar between PV and left atrium cardiomyocytes [29]. Because PV cardiomyocytes have less negative resting membrane potential and smaller I_{K1} [7,30], the activation of the reverse mode of NCX with an increase in the SR Ca^{2+} content will lead to diastolic Ca^{2+} release and activate the forward mode of NCX with the genesis of DADs and arrhythmias.

It has been shown that KB-R7943 increased the APD in cardiomyocytes [23,24]. Consistently, our results showed that KB-R7943 prolonged APD in the PVs. The reduction in the reverse mode of NCX and potassium currents by KB-R7943 may contribute to the prolongation of the APD. This effect may prevent the genesis of microreentry in the PVs which has been proposed to be one of the mechanisms of PV arrhythmogenicity [31].

4.2. Role of NCX inhibitors in the ouabain-induced arrhythmogenicity

Ouabain-induced arrhythmogenesis is a frequently used model in studying triggered activity-induced cardiac arrhythmias. In this study, we demonstrated that ouabain not only increased the firing rates in the PVs with spontaneous activity but also induced arrhythmogenic activity in the non-spontaneous firing PVs. Ouabain may increase the PV firing rates through the increase of intracellular Ca^{2+} due to the increase of intracellular Na^+ and the decrease of Na^+ gradient and Ca^{2+} extrusion. In contrast to that observed by Honjo et al. [13], this study demonstrated the occurrence of phase 4 depolarization in the PV tissue preparations, which suggested that increased automaticity and triggered activity are the underlying mechanisms of ouabain-induced PV arrhythmogenesis. Moreover, the higher inducible arrhythmogenesis in the PVs than in the atrial tissue suggested a high arrhythmogenic potential of the PVs.

Previous studies have found that KB-R7943 may prevent glycoside-induced atrial and ventricular arrhythmias [23,24]. In this study, we demonstrated that pretreatment with KB-R7943 prevented the arrhythmogenic activity of ouabain on the PV cardiomyocytes and also prevented the APD shortening by ouabain. The beneficial effects of KB-R7943 may be due to a reduction in the intracellular Ca^{2+}. However, similar to the previous study [32], KB-R7943 did not affect the inotropic effect of cardiac glycosides and did not terminate the ouabain-induced PV arrhythmogenesis. This could be explained by the fact that KB-R7943 did not counteract the inhibition of the Na^+/K^+-ATPase by ouabain. If ouabain toxicity had progressed sufficiently, the reduction in Ca^{2+} entry through the reverse mode of NCX may not be able to decrease the Ca^{2+} overload of the SR.

5. Conclusions

This study demonstrated that NCX currents may play a role in the PV electrical activity through a reduction in the SR Ca^{2+} content. KB-R7943 reduces the PV arrhythmogenenic activity and prevents the ouabain-induced PV arrhythmogenesis. These findings suggest that KB-R7943 may have a potential role in treating AF.

Acknowledgements

The present work was supported by grants NSC 94-2314-B-075-093, NSC 94-2314-B-010-056, NSC 94-2314-B-010-053, VGH 94-204, VGH 94-005, VGH 94-206, VGH 94-009, SKH-TMU-94-01 from Shin Kong Wu Ho-Su Memorial Hospital and MMH E-94003 from Mackay Memorial Hospital.

References

[1] Haissaguerre M, Jais P, Shah DC, Takahashi A, Hocini M, Quiniou G, et al. Spontaneous initiation of atrial fibrillation by ectopic beats originating in the pulmonary veins. N Engl J Med 1998;339:659–66.

[2] Chen SA, Hsieh MH, Tai CT, Tsai CF, Prakash VS, Yu WC, et al. Initiation of atrial fibrillation by ectopic beats originating from the pulmonary veins: electrophysiological characteristics, pharmacological responses, and effects of radiofrequency ablation. Circulation 1999;100:1879–86.
[3] Jais P, Hocini M, Macle L, Choi KJ, Deisenhofer I, Weerasooriya R, et al. Distinctive electrophysiological properties of pulmonary veins in patients with atrial fibrillation. Circulation 2002;106:2479–85.
[4] Blom NA, Gittenberger-de Groot AC, DeRuiter MC, Poelmann RE, Mentink MM, Ottenkamp J. Development of the cardiac conduction tissue in human embryos using HNK-1 antigen expression: possible relevance for understanding of abnormal atrial automaticity. Circulation 1999;99:800–6.
[5] Perez-Lugones A, McMahon JT, Ratliff NB, Saliba WI, Schweikert RA, Marrouche NF, et al. Evidence of specialized conduction cells in human pulmonary veins of patients with atrial fibrillation. J Cardiovasc Electrophysiol 2003;14:803–9.
[6] Chen YJ, Chen SA, Chang MS, Lin CI. Arrhythmogenic activity of cardiac muscle in pulmonary veins of the dog: implication for the genesis of atrial fibrillation. Cardiovasc Res 2000;48:265–73.
[7] Chen YJ, Chen SA, Chen YC, Yeh HI, Chan P, Chang MS, et al. Effects of rapid atrial pacing on the arrhythmogenic activity of single cardiomyocytes from pulmonary veins: implication in initiation of atrial fibrillation. Circulation 2001;104:2849–54.
[8] Chen YJ, Chen SA, Chen YC, Yeh HI, Chang MS, Lin CI. Electrophysiology of single cardiomyocytes isolated from rabbit pulmonary veins: implication in initiation of focal atrial fibrillation. Basic Res Cardiol 2002;97:26–34.
[9] Hocini M, Ho SY, Kawara T, Linnenbank AC, Potse M, Shah D, et al. Electrical conduction in canine pulmonary veins: electrophysiological and anatomic correlation. Circulation 2002;105:2442–8.
[10] Chen PS, Wu TJ, Hwang C, Zhou S, Okuyama Y, Hamabe A, et al. Thoracic veins and the mechanisms of non-paroxysmal atrial fibrillation. Cardiovasc Res 2002;54:295–301.
[11] Chen YC, Chen SA, Chen YJ, Chang MS, Chan P, Lin CI. Effects of thyroid hormone on the arrhythmogenic activity of pulmonary vein cardiomyocytes. J Am Coll Cardiol 2002;39:366–72.
[12] Kimura J, Miyamae S, Noma A. Identification of sodium-calcium exchange current in single ventricular cells of guinea-pig. J Physiol 1987;384:199–222.
[13] Honjo H, Boyett MR, Niwa R, Inada S, Yamamoto M, Mitsui K, et al. Pacing-induced spontaneous activity in myocardial sleeves of pulmonary veins after treatment with ryanodine. Circulation 2003;107:1937–43.
[14] Patterson E, Po SS, Scherlag BJ, Lazzara R. Triggered firing in pulmonary veins initiated by in vitro autonomic nerve stimulation. Heart Rhythm 2005;2:624–31.
[15] Watano T, Kimura J, Morita T, Nakanishi H. A novel antagonist, No. 7943, of the Na^+/Ca^{2+} exchange current in guinea-pig cardiac ventricular cells. Br J Pharmacol 1996;119:555–63.
[16] Iwamoto T, Watano T, Shigekawa M. A novel isothiourea derivative selectively inhibits the reverse mode of Na^+/Ca^{2+} exchange in cells expressing NCX1. J Biol Chem 1996;271:22391–7.
[17] Elias CL, Lukas A, Shurraw S, Scott J, Omelchenko A, Gross GJ, et al. Inhibition of Na^+/Ca^{2+} exchange by KB-R7943: transport mode selectivity and antiarrhythmic consequences. Am J Physiol Heart Circ Physiol 2001;281:H1334–45.
[18] Seki S, Taniguchi M, Takeda H, Nagai M, Taniguchi I, Mochizuki S. Inhibition by KB-R7943 of the reverse mode of the Na^+/Ca^{2+} exchanger reduces Ca^{2+} overload in ischemic-reperfused rat hearts. Circ J 2002;66:390–6.
[19] Miyata A, Zipes DP, Hall S, Rubart M. KB-R7943 prevents acute, atrial fibrillation-induced shortening of atrial refractoriness in anesthetized dogs. Circulation 2002;106:1410–9.
[20] Sticherling C, Oral H, Horrocks J, Chough SP, Baker RL, Kim MH, et al. Effects of digoxin on acute, atrial fibrillation-induced changes in atrial refractoriness. Circulation 2000;102:2503–8.
[21] Tieleman RG, Blaauw Y, Van Gelder IC, De Langen CD, de Kam PJ, Grandjean JG, et al. Digoxin delays recovery from tachycardia-induced electrical remodeling of the atria. Circulation 1999;100:1836–42.
[22] Cheung DW. Pulmonary vein as an ectopic focus in digitalis-induced arrhythmia. Nature 1981;294:582–4.
[23] Satoh H, Ginsburg KS, Qing K, Terada H, Hayashi H, Bers DM. KB-R7943 block of Ca^{2+} influx via Na^+/Ca^{2+} exchange does not alter twitches or glycoside inotropy but prevents Ca^{2+} overload in rat ventricular myocytes. Circulation 2000;101:1441–6.
[24] Watano T, Harada Y, Harada K, Nishimura N. Effect of Na^+/Ca^{2+} exchange inhibitor, KB-R7943 on ouabain-induced arrhythmias in guinea-pigs. Br J Pharmacol 1999;127:1846–50.
[25] Chen YJ, Chen YC, Tai CT, Yeh HI, Lin CI, Chen SA. Angiotensin II and angiotension II receptor blocker modulate the arrhythmogenic activity of pulmonary vein. Br J Pharmacol 2006;147:12–22.
[26] Scoote M, Williams AJ. Myocardial calcium signalling and arrhythmia pathogenesis. Biochem Biophys Res Commun 2004;322:1286–309.
[27] Schotten U, Greiser M, Benke D, Buerkel K, Ehrenteidt B, Stellbrink C, et al. Atrial fibrillation-induced atrial contractile dysfunction: a tachycardiomyopathy of a different sort. Cardiovasc Res 2002;53:192–201.
[28] Maltsev VA, Vinogradova TM, Bogdanov KY, Lakatta EG, Stern MD. Diastolic calcium release controls the beating rate of rabbit sinoatrial node cells: numerical modeling of the coupling process. Biophys J 2004;86:2596–605.
[29] Melnyk P, Ehrlich JR, Pourrier M, Villeneuve L, Cha TJ, Nattel S. Comparison of ion channel distribution and expression in cardiomyocytes of canine pulmonary veins versus left atrium. Cardiovasc Res 2005;65:104–16.
[30] Ehrlich JR, Cha TJ, Zhang L, Chartier D, Melnyk P, Hohnloser SH, et al. Cellular electrophysiology of canine pulmonary vein cardiomyocytes: action potential and ionic current properties. J Physiol 2003;551:801–13.
[31] Chou CC, Nihei M, Zhou S, Tan A, Kawase A, Macias ES, et al. Intracellular calcium dynamics and anisotropic reentry in isolated canine pulmonary veins and left atrium. Circulation 2005;111:2889–97.
[32] Miyamoto S, Zhu BM, Kamiya K, Nagasawa Y, Hashimoto K. KB-R7943, a Na^+/Ca^{2+} exchange inhibitor, does not suppress ischemia/reperfusion arrhythmias nor digitalis arrhythmias in dogs. Jpn J Pharmacol 2002;90:229–35.